SUPPLEMENTAL MATERIAL

Mukherjee et al., https://doi.org/10.1084/jem.20161134

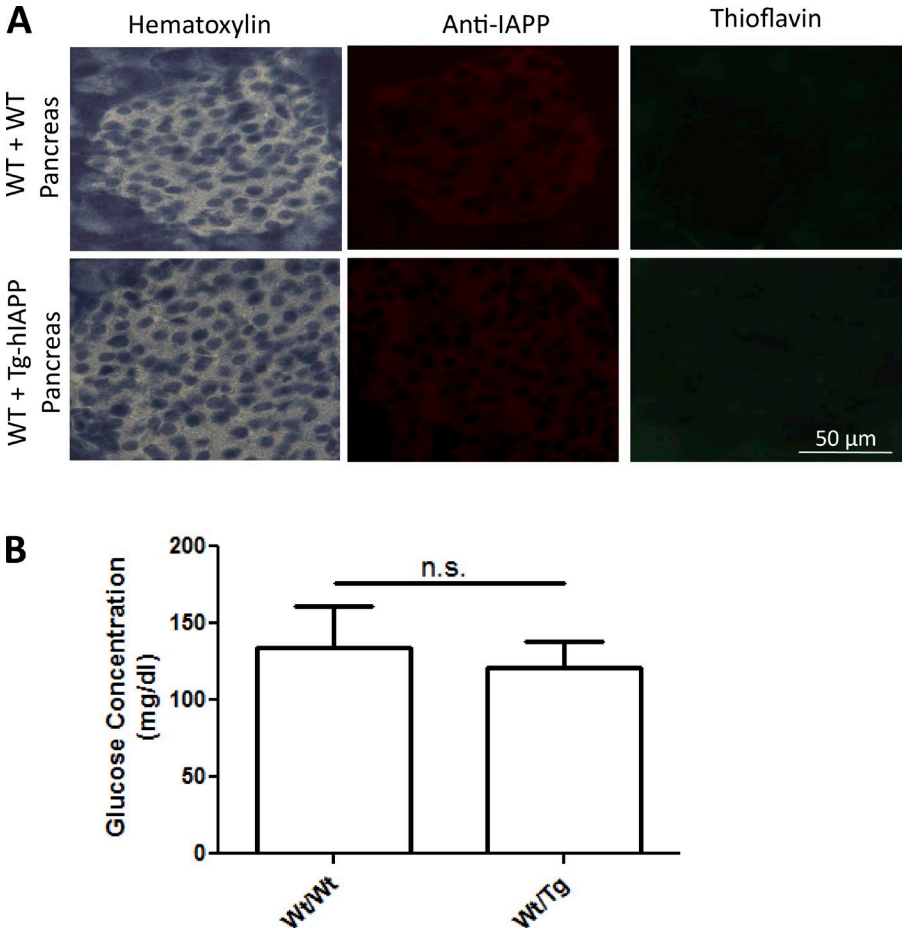

Figure S1. **WT mice inoculated with T2D Tg pancreas homogenates do not develop IAPP deposits or hyperglycemia.** As controls of the experiments shown in Figs. 2 and 3, groups of 3-wk-old WT mice were inoculated with 10% pancreas homogenate from 12-mo-old Tg-hIAPP mice or non-Tg littermates. Animals were sacrificed at 10 wk old, and the pancreata were fixed and used for histologic analysis (A). Hematoxylin and thioflavin staining, as well as immunohistochemistry with anti-IAPP antibody, did not show any indication of accumulation of IAPP deposits. This result indicates that the amyloid staining observed in Fig. 2 was not coming from the inoculum material but, rather, from accumulation of endogenously produced IAPP aggregates. (B) Before animals were sacrificed, fasting blood was taken to measure glucose, as described in the Materials and methods. No hyperglycemia was observed in these animals. The values correspond to the means ± SE of the five animals studied. Differences were not statistically significant, as analyzed by unpaired *t* test (P = 0.39).

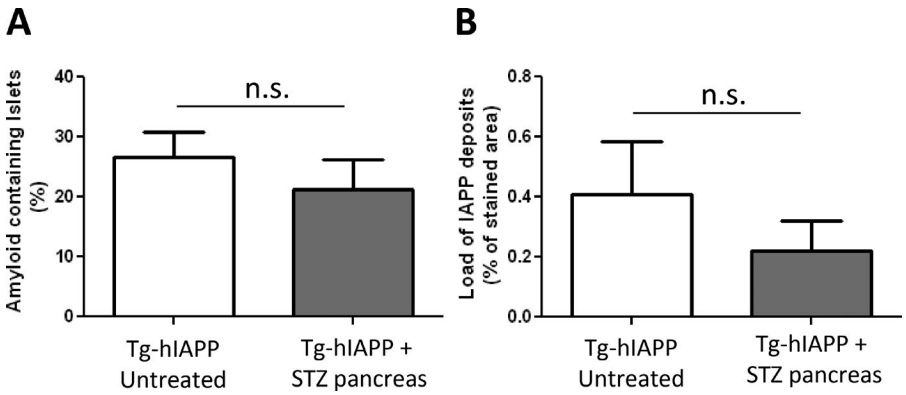

Figure S2. **Injection of pancreas homogenates from STZ-induced diabetic mice does not affect IAPP aggregation.** WT mice were induced to develop hyperglycemia by injection of STZ as described in Materials and methods. Pancreas homogenates from these animals were used to inject i.p. into young (3-wk-old) Tg-hIAPP mice. Animals were sacrificed at 16 wk old, along with untreated animals of the same age, andpancreata were collected to analyze the presence of IAPP aggregates by staining with anti-IAPP antibodies or ThS. Image analysis of the immunohistochemical studies was performed to estimate the percentage of islets containing amyloid deposits (A) and the load of IAPP aggregates (B), calculated as the percentage of the stained area compared with the total islet area. The values correspond to the means ± SE of the results obtained for the five animals used per each group. The data were analyzed by unpaired *t* test, and no significant differences were found. (A) P = 0.42; (B) P = 0.35.

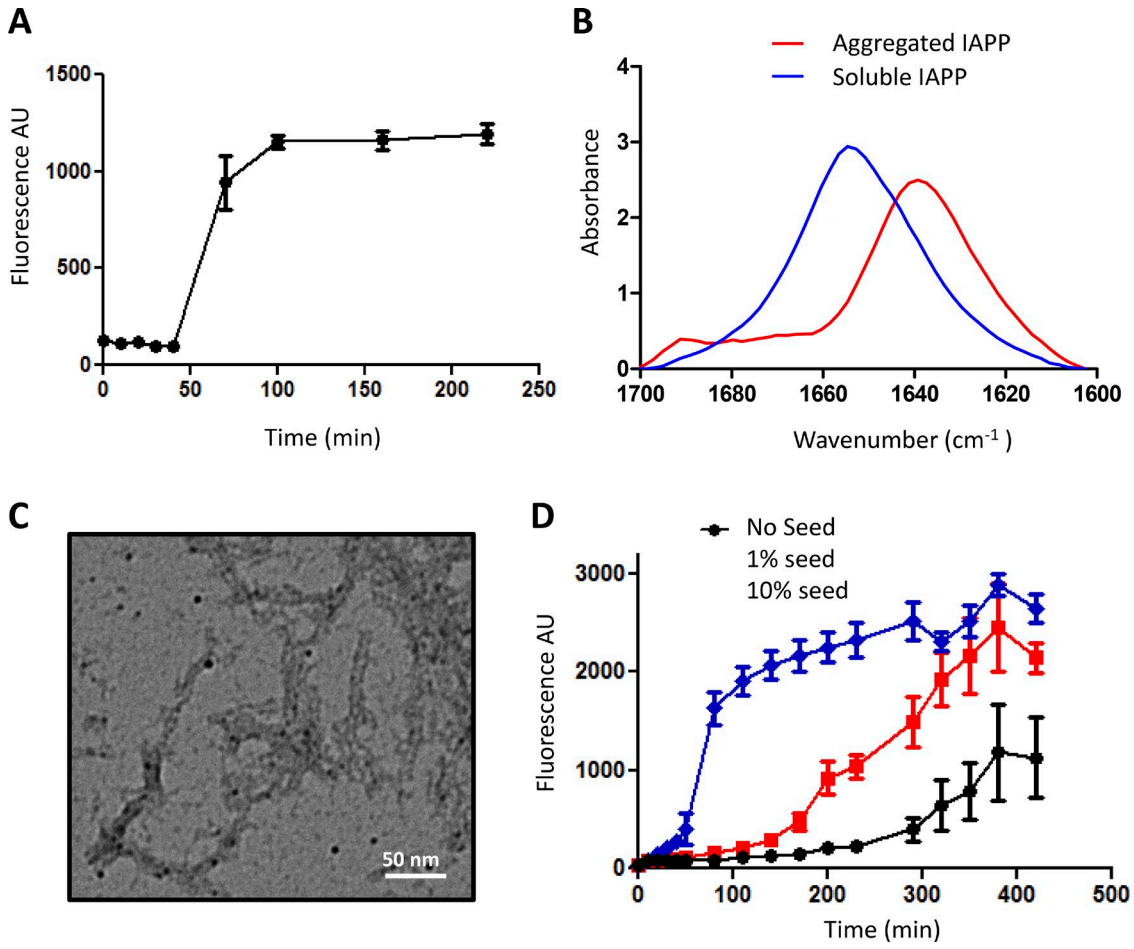

Figure S3. **Preparation and characterization of synthetic IAPP aggregates in vitro.** (A) Amyloid formation from freshly prepared, soluble hIAPP (0.2 mg/ml final concentration) was measured, at different times, by ThT binding assay. Each point represents means ± SE from five replicates. AU, arbitrary units. (B) FTIR spectroscopy studies of the secondary structure of soluble (blue line) and aggregated (red line) IAPP. (C) Electron microscopy images of negatively stained aliquots of aggregated material, examined using a magnification of 150,000, indicated typical fibrillar morphology. (D) To test seeding potential, different quantities of newly formed aggregates were added in standard IAPP aggregation assay, monitored by ThT binding. Each point represents means ± SE of five individual measurements. The final IAPP concentration in this assay was 0.1 mg/ml, which explains the longer lag time compared with the graph in A.

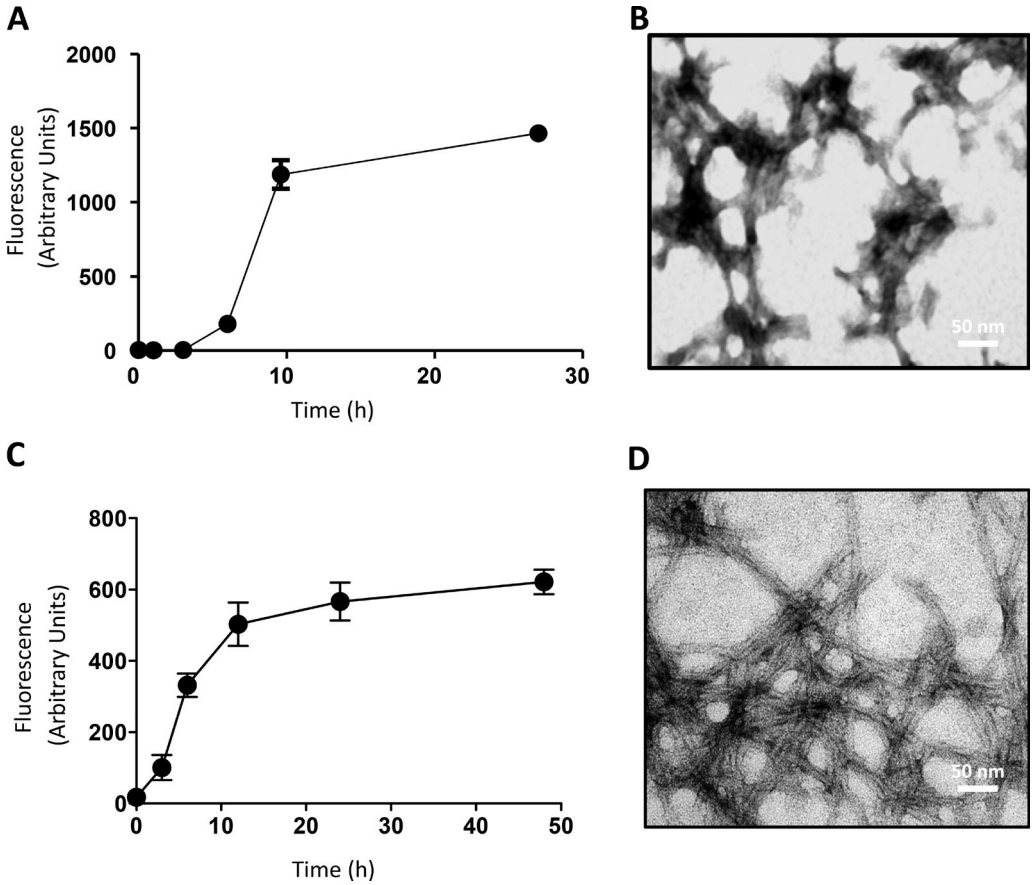

Figure S4. **Production and characterization of Tau and Mcc fibrillar aggregates in vitro.** To use them as specificity controls in experiments described in Tau (Fig. 5, A and B) and Mcc (Fig. 5, C and D) aggregates were produced. K18 Tau aggregates were prepared by intermittent shaking (500 rpm) of 50 µM purified recombinant protein at 37°C in 100 mM Hepes, pH 7.4, containing 100 mM NaCl and 25 µM heparin. Mcc aggregates were prepared by constant shaking (500 rpm) of 100 µM purified protein at 37°C in 50 mM Pipes, pH 6.5, containing 500 mM NaCl. Amyloid formation was followed by the ThT assay (A and C) and transmission electron microscopy (B and D). Error bars in A and C correspond to SE.